

# A Low-Noise Amplifier at 77 GHz in SiGe:C Bipolar Technology

Bernhard Dehlink<sup>1,2</sup>, Hans-Dieter Wohlmuth<sup>2</sup>,  
Klaus Aufinger<sup>2</sup>, Thomas F. Meister<sup>2</sup>, Josef Böck<sup>2</sup>, Arpad L. Scholtz<sup>1</sup>

<sup>1</sup>Technical University of Vienna, Gusshausstrasse 25, A-1040 Vienna, Austria

<sup>2</sup>INFINEON Technologies AG, Corporate Research,  
Otto-Hahn-Ring 6, D-81739 Munich, Germany  
bernhard.dehlink@infineon.com

*Abstract – A single ended low noise amplifier at 77 GHz has been designed, implemented, and characterized. The focus was on a low noise figure, reasonable input and output matching, and a high input compression point which are basic requirements for automotive radar applications or car-to-car communication systems. The LNA was fabricated in a 225 GHz ft SiGe:C bipolar technology. At 77 GHz, the measured gain of the LNA is 8.9 dB, and the measured noise figure at 77 GHz is 4.8 dB. The measured input compression point at 77 GHz is -3 dBm. The circuit was designed for a supply voltage of 5.5 V and draws 22 mA.*

*Keywords:* Low Noise Amplifier, Millimeter Wave, Si-Ge, Bipolar, Automotive

## I. INTRODUCTION

Advances in Silicon-Germanium bipolar technology lead to a deeper involvement in highest frequency applications, like automotive radar at a frequency range from 76 GHz to 77 GHz, car-to-car communication, or wireless communication systems at the Industrial, Scientific, Medical (ISM) band from 59 GHz to 64 GHz. Many interesting publications show the demand for this technology in the millimeter wave range [1], [2], [3]. Different building blocks, including voltage-controlled oscillators, mixers, and amplifiers have been published at various frequencies [2], [4], [5], [6]. In this work, a single-ended low noise amplifier for an automotive radar system has been designed, implemented, and measured. The other building blocks of the system have already been published: a powerful VCO [4], and a fully differential mixer[6]. One important aspect was the compatibility with these components. This paper presents the design and the measured results in detail.

## II. TECHNOLOGY

The LNA was implemented in an advanced 225 GHz ft SiGe:C bipolar technology, based on the technology presented in [7]. The maximum oscillation frequency  $f_{\max}$  is 300 GHz. Shallow and deep trench isolation are used. The transistors are fabricated with a double-polysilicon

self-aligned emitter base configuration with a SiGe:C base. This base is integrated by selective epitaxial growth. The technology uses a  $0.3 \mu\text{m}$  lithography. The minimum effective emitter width is  $0.14 \mu\text{m}$ . The breakdown voltage of the HBTs at open base is 1.8 V. This technology provides four metal layers, MIM-capacitors, and different types of resistors.

We use metal layer four over metal layer two for the design of the transmission lines. A  $5 \mu\text{m}$  wide metal four signal path over a metal two ground path yields a  $50 \Omega$  microstrip line. The maximum width of metal two is limited to  $15 \mu\text{m}$ , but a cheersed structure was used to expand the ground plane. The transmission lines were modeled with a Matlab tool based on a 2D field simulator. Simulations show that the transmission lines have a loss of 1 dB per millimeter, and an effective dielectric constant of 3.9 at 77 GHz.

## III. CIRCUIT DESIGN

To be compatible with other building blocks, a voltage supply of 5.5 V had to be used. Since single ended antennas are commonly used, the topology of the LNA was chosen to be of the same type. Therefore losses introduced by baluns, resulting in noise figure degradation, can be avoided. Additionally, fully differential measurement equipment is not available at those frequencies. The schematic of the LNA is depicted in Figure 1.

A good trade-off between power and noise matching must be achieved. Simulations showed that good power matching resulted in a noise figure degradation of only 0.5 dB above the minimum noise figure, thus we concluded to focus on this aspect. The matching stages consist of the  $50 \Omega$  transmission lines described in the previous section. An open stub and a series microstrip line are employed at both the input and the output of the circuit. In Figure 1, the matching structures are labeled  $T_1, T_2$  at the input and  $T_4, T_5$  at the output. The low-noise amplifier consists of two common-emitter stages. The base-emitter biasing is done by a current mirror where we placed a resistor ( $R_2, R_3$ ) between the bases to decouple the biasing circuit from the high frequency path. We chose the sizes of the transistors to minimize the noise figure, thus the current density ( $1.57 \text{mA}/\mu\text{m}^2$ ) is below the value for maximum  $f_T$  ( $6 \text{mA}/\mu\text{m}^2$ ) [7]. At the input

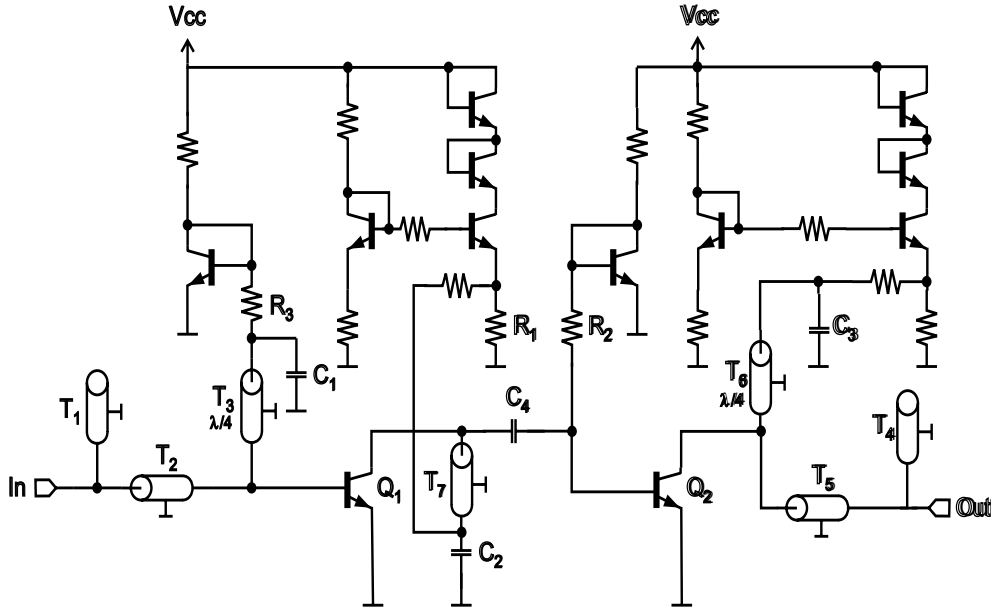


Fig. 1. Schematic diagram of the LNA.

of the first stage, the quarter-wavelength transformer  $T_3$  decouples the reference side of the current mirror from the signal path. The MIM-capacitor  $C_1$  has a value of 4 pF to provide good AC-ground. Maximum signal power transfer between the two stages was met by using an LC matching network, consisting of  $T_7$  and  $C_4$ . The transmission line is shorted versus ground by the capacitor  $C_2$  (3 pF). This, together with the series resistor, ensures stability.

The high supply voltage of 5.5 V requires additional measures to prevent the collector-emitter voltage from exceeding the breakdown voltage level. A breakdown would cause a significant rise in the noise figure. A voltage divider, an emitter follower, and the resistor  $R_1$  keep the voltage at the collector at a constant level.

In the second stage, the resistor  $R_2$  has a value of  $500\Omega$ . Its purpose is the decoupling of the reference path of the current mirror from the signal path. At the output of the common-emitter stage, decoupling is achieved by a quarter-wavelength transmission line. This line transforms the impedance of the capacitor  $C_3$  (4 pF) to a high impedance level. The same method like in the first stage is used to achieve a constant DC-level at the collector of  $Q_2$ .

#### IV. EXPERIMENTAL RESULTS

Figure 2 shows a photograph of the fabricated LNA. The matching structures, the quarter-wavelength transformers, and the MIM capacitors occupy the majority of the chip area. The S-parameters were measured using millimeter-wave probes. The temperature of the device was kept at a constant level of  $25^\circ\text{C}$  for all measurements. For the on-wafer measurements, we used 120 GHz

Ground-Signal-Ground (GSG) and 120 GHz GS probes from Picoprobe. The noise figure was measured using HP's 8970B noise figure meter. The noise source was NoiseCom's NC5110. Due to the high ENR values (15 dB), an isolator was used to improve the matching. We used HP's 83650A synthesizer and the HP83558A W-band frequency extender for the local oscillator. The compression point was measured using the same synthesizer (HP 83650A) and the same frequency extender (HP83558A) at the input of the LNA. HP's 8565EC spectrum analyzer and the HP frequency extender for the W-band (HP 11970W) were used at the output. For this measurement, we had to attach an attenuator to the output of the LNA to ensure an offset of 10 dB to the compression point of the extender HP 11970W. To connect the devices, W-band waveguides of various lengths were used.

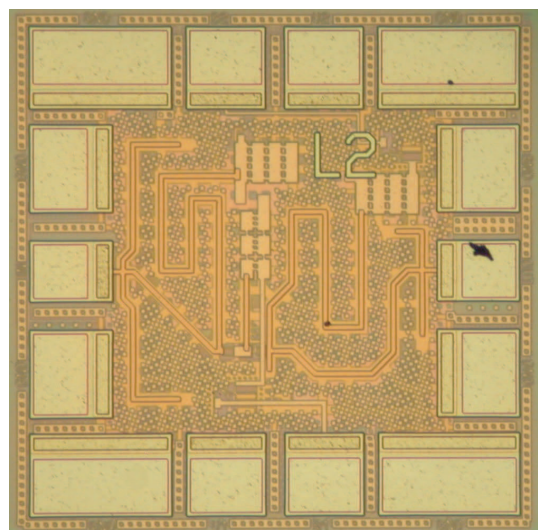


Fig. 2. Die photograph of the LNA. Die size is  $0.45 \times 0.45\text{mm}^2$

The measured input and output matching and the measured gain are depicted in Figure 3. The LNA is matched very well from 70 GHz up to 87 GHz, which is in excellent agreement with the simulation results. At 77 GHz, S<sub>11</sub> reads -26 dB, and S<sub>22</sub> is at -19 dB.

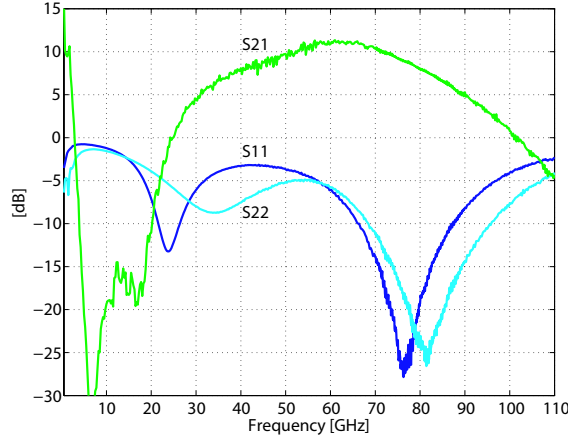


Fig. 3. Measured S-parameters.

The noise figure of the LNA was measured using an active mixer. This mixer is similar to the Gilbert-cell mixer presented in [6]. From the measurements of the stand-alone mixer and of the combination, it is possible to calculate the noise figure using

$$F_{LNA} = \frac{1}{2} \left[ F_{DSB,DUT} - \frac{1}{G_{LNA}} (F_{DSB,MIX} - 2) \right], \quad (1)$$

where  $F_{DSB,DUT}$  is the measured double sideband noise figure of the combined LNA and mixer circuit,  $F_{DSB,MIX}$  is the measured double sideband noise figure of the mixer, and  $G_{LNA}$  and  $F_{LNA}$  are the gain and the noise figure of the LNA, respectively. The difference to Friis' formula comes from the double sideband noise figure since the signal is located in one sideband only. An intermediate frequency of 10 MHz was chosen, so no image frequency filter could be used. The de-embedded noise figure and the de-embedded gain are depicted in Figure 4. The noise figure remains lower than 5.5 dB over a frequency range from 75 GHz to 87 GHz. At the desired frequency of 77 GHz, the noise figure is 4.8 dB, and the gain is 8.3 dB. From Figure 3, S<sub>21</sub> reads 8.9 dB at this frequency. These values are 4 dB lower than simulated. The difference results from the non-ideal quality factor of the decoupling capacitor C<sub>4</sub>. This behavior was verified by simulations. Although an isolator was used at the input, the unmatched noise source, waveguide connections, and the transition from the waveguide to the probes causes a variation in the noise figure over the frequency of  $\pm 0.5$  dB.

A plot of the gain versus input power at 77 GHz is depicted in Figure 5. The input 1 dB compression point is -3 dBm.

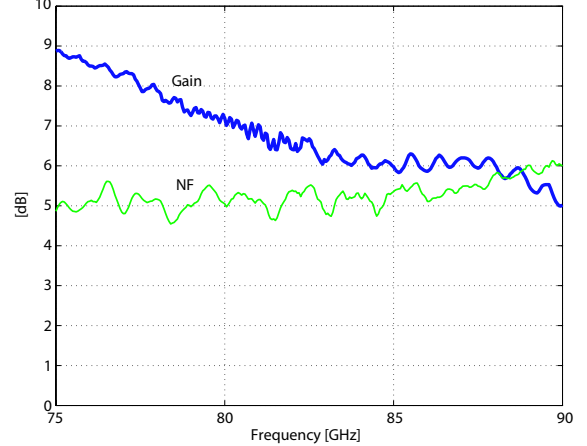


Fig. 4. Measured Noise Figure and Gain of the LNA.

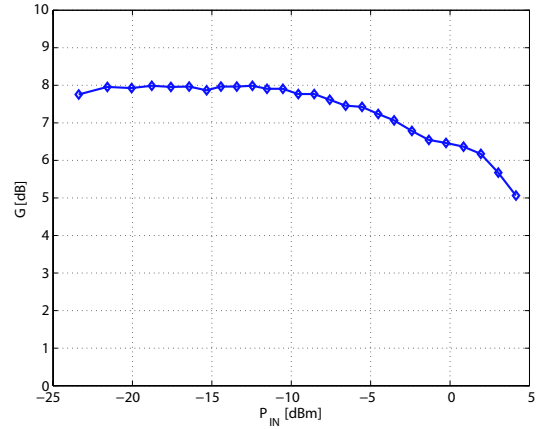


Fig. 5. Measured Gain Compression at 77 GHz

## V. CONCLUSION

A single-ended low noise amplifier was designed in a SiGe:C bipolar technology and characterized. The measured results are summarized in Table I. For comparison purposes, other LNAs in SiGe and III-V technologies are listed as well as LNAs at other frequencies. All displayed values are measured results, except marked by (sim.).

The comparison shows that the LNA presented in this work exhibits state of the art performance. The input compression point is at a high level, 7 dB higher than in other state of the art circuits. The noise figure remains below 5.5 dB over a wide frequency range, while the gain is at an acceptable level of 8.9 dB. Thus, this LNA can be used in environments where a high dynamic operating range is needed, for example in automotive radar systems or in car-to-car communication systems.

## VI. ACKNOWLEDGEMENT

This work was supported by the German Bundesministerium für Bildung und Forschung (BMBF) under contract 10 M3161A (KOKON).

TABLE I  
PERFORMANCE SUMMARY AND COMPARISON WITH OTHER LNAs

	This Work	[2]	[8]	[5]	[9]	[10]
Technology	SiGe:C $f_T = 225 \text{ GHz}$	SiGe $f_T = 200 \text{ GHz}$	SiGe $f_T = 200 \text{ GHz}$	SiGe $f_T = 160 \text{ GHz}$	GaAs pHEMT -	GaAs MHEMT $f_T = 290 \text{ GHz}$
Target Frequency [GHz]	77	77	60	52	77	90
Noise Figure [dB]	5.5	5.6 (sim.)	4.5	-	4	3
S11 [dB]	-26	-10	-6	-12	-7	-12
S22 [dB]	-19	-21	-17	-6	-7	-15
S21 [dB]	8	15	15	22.7	10	19
S12 [dB]	-33	-40	-40	-30	-33	-
iCP <sub>1dB</sub> [dBm]	-3	-17	-20	-	-	-10
Supply voltage [V]	5.5	1.8	1.8	3.3	3.0	1.5
DC-current [mA]	22	8	6	11.4	30	24
Chip size [mm <sup>2</sup> ]	$0.45 \times 0.45$	-	$0.9 \times 0.6$	$0.35 \times 0.450$	$1.34 \times 1.0$	$1.0 \times 3.0$

## VII. REFERENCES

- [1] W. Winkler, J. Borngräber, H. Gustat, and F. Korndörfer, “60 GHz Transceiver Circuits in Si-Ge:C BiCMOS Technology,” in *Proceedings of the 30<sup>th</sup> European Solid-State Circuits Conference*. IEEE, September 2004, pp. 83–86.
- [2] B. Floyd, “V-Band and W-Band SiGe Bipolar Low-Noise Amplifiers and Voltage-Controlled Oscillators,” in *Radio Frequency Integrated Circuits (RFIC) Symposium*. IEEE, June 2004, pp. 295–298.
- [3] D. Bryant, R. Eye, J. Carroll, and D. Allen, “Integrated LNA-sub-harmonic mixer for 77 GHz automotive radar applications using GaAs pHEMT technology,” in *Compound Semiconductor Integrated Circuit Symposium*. IEEE, October 2004, pp. 257 – 259.
- [4] H. Li, H.-M. Rein, T. Suttorp, and J. Böck, “Fully integrated SiGe VCOs with powerful output buffer for 77-GHz automotive Radar systems and applications around 100 GHz,” in *IEEE International Solid State Circuits Conference*, vol. 39, no. 10, October 2004, pp. 1650 – 1658.
- [5] M. Gordon and P. Voinigescu, “An Inductor-Based 52 GHz  $0.18 \mu\text{m}$  SiGe HBT Cascode LNA with 22 dB Gain,” in *ESSCIRC*. IEEE, September 2004, pp. 287–290.
- [6] W. Perndl, H. Knapp, M. Wurzer, K. Aufinger, T. Meister, J. Böck, W. Simbürger, and A. Scholtz, “A low-noise, and high-gain double-balanced mixer for 77 GHz automotive radar front-ends in SiGe bipolar technology,” in *Radio Frequency Integrated Circuits Symposium*. IEEE, June 2004, pp. 47–50.
- [7] J. Böck, H. Schäfer, H. Knapp, K. Aufinger, M. Wurzer, S. Boguth, T. Böttner, R. Stengl, W. Perndl, and T. Meister, “3.3 ps SiGe Bipolar Technology,” in *Electron Devices Meeting, IEEE. IEDM Technical Digest*, December 2004, pp. 255–258.
- [8] B. Floyd, S. Reynolds, U. Pfeiffer, T. Zwick, T. Beukema, and B. B. Gaucher, “SiGe bipolar transceiver circuits operating at 60 GHz,” *Solid-State Circuits*, vol. 40, no. 1, pp. 156 – 167, January 2005.
- [9] R. Eye and D. Allen, “77 GHz low noise amplifier for automotive radar applications,” in *Gallium Arsenide Integrated Circuit (GaAs IC) Symposium*. IEEE, November 2003, pp. 139 – 142.
- [10] C. Schwörer, A. Tessmann, A. Leuther, H. Massler, W. Reinert, and M. Schlechtweg, “Low Noise W-Band Amplifiers for Radiometer Applications Using a 70nm Metamorphic HEMT Technology,” in *11th GAAS Symposium*. Munich: IEEE, 2003, pp. 373 – 376.